Solid-State Electronics Vol. 24, pp. 533–538, 1981
Printed in Great Britain.

0038–1101/81/060533–06$02.00/0
Pergamon Press Ltd.

HIGH-LOW JUNCTIONS FOR SOLAR CELL APPLICATIONS

J. DEL ALAMO
Instituto de Energía Solar, Universidad Politécnica de Madrid, Spain

and

J. VAN MEERBERGEN†, F. D'HOORE and J. NIJS
Lab. E.S.A.T., Dept. Elektrotechniek, Katholieke Universiteit Leuven, Heverlee, Belgium

(*Received* 29 *January* 1980, *in revised form* 28 *July* 1980)

Abstract—A new theoretical model to calculate the effective surface recombination velocity (S_{eff}) of a high–low junction with an arbitrary impurity distribution is presented. The model is applied to erfc-diffused pp^+ junctions using experimental data of bandgap narrowing, lifetime and mobility. Bandgap narrowing is shown to degrade the minority carrier reflecting properties of the high–low junction. Computer results are applied for the design of BSF solar cells and to study other solar cell structures based on high–low junctions.

NOTATION

- D diffusivity of minority carriers
- D_e diffusivity of electrons in a p^+ region
- J minority carrier current
- J_e electron current in a p^+ region
- k Boltzmann constant
- L minority carrier diffusion length
- n electron concentration
- n' excess electron concentration
- n_{ie} effective intrinsic carrier concentration
- n_{io} intrinsic carrier concentration
- n_0 equilibrium electron concentration
- N_A acceptor concentration
- N_{Aeff} effective acceptor concentration
- N_B base concentration
- N_{Beff} effective base concentration
- N_{eff} effective impurity concentration
- p hole concentration
- q electron charge
- S defined in eqn (9)
- S_b back surface recombination velocity
- S_e defined in eqn (9)
- S_{eff} effective surface recombination velocity of the high–low junction
- T absolute temperature
- W heavily-doped region thickness
- x unit of length
- α_T minority carrier transport factor
- τ minority carrier lifetime
- τ_e electron lifetime

1. INTRODUCTION

Theoretical studies[1–3] and experimental results[4–6] have shown the beneficial influence of the high–low junction at the back side of a solar cell. The reflection of minority carriers at the high–low junction can be modelled by an effective surface recombination velocity. The improvement in open circuit voltage and short-circuit current of BSF cells has been explained using this concept[1]. Design criteria of this highly doped layer at the back side is available from exact computer simulations when the back surface is totally covered by a good ohmic contact[2, 3].

Recently the use of high–low junctions on illuminated surfaces has been proposed to reduce the surface recombination velocity. High efficiencies can be obtained with the High-Low Emitter Solar Cell[7, 8], the Double Sided Surface Field Cell[9] and the Front Surface Field Solar Cell[10]. In order to maximize the photovoltaic response of a solar cell the junction depth of a high–low junction at the front side has to be minimized. Hence the set of parameter values of conventional BSF design cannot be used on these new devices. The impurity concentration at the surface and the surface recombination velocity together with the junction depth must now be carefully choosen to obtain an effective collection efficiency in combination with a high open-circuit voltage.

Previous models of the BSF effect considered abrupt high–low junctions and derived a simple formula for the effective surface recombination velocity which explained the early successful results[1]. The simplified model, developed for the first Al-alloyed structures, is still used for the actual deep diffused profiles[11, 12]. Exact computer simulations that solve the six Shockley equations have already included more realistic erfc profiles with a position dependent lifetime[2]. Heavy doping effects are included by using rigid bandgap narrowing models. Using such computer simulations the different physical mechanisms underlying the operation of the high–low junction are difficult to separate and the importance of certain parameters can easily be shadowed.

In this paper a new simple one-dimensional analysis of the high–low junction is presented. This model can be applied to an arbitrary profile and includes mobility and lifetime that are position dependent. It considers heavy doping effects and a finite surface recombination velocity. Usually some approximations are allowed and simple formulae can be derived. Design criteria for the three afore-mentioned new structures are considered. Also the case of partial coverage of the back contact by an oxide is studied since this has been recently proposed as a method to increase the short-circuit current of BSF

†Present address: Philips Research Laboratories, Eindhoven, The Netherlands.

cells[13]. The results of this simple modelling are compared with exact computer simulations, solving the six Shockley equations.

The paper proceeds as follow. Section 2 develops a theoretical model to calculate the effective surface recombination velocity of a given profile. A simple differential equation is derived to take into account the three main physical mechanisms affecting minority carriers: diffusion, drift and recombination. Two particular interesting cases are studied: abrupt junction and transparent layer (recombination only at the back contact). Simple equations are derived for both cases. Section 3 solves the differential equation derived in Section 2 for some particular cases. The main physical mechanism are identified and their influence is explained. In Section 4 design criteria for BSF solar cells are revised. High–low junctions on illuminated front layers are studied. The diffusion parameters for an optimum operation are established. Section 5 summarizes the main conclusions of the paper.

2. THEORETICAL MODEL

It is well known that the presence of a back surface field in a solar cell lowers the dark injection current into the bulk and thus enhances the open-circuit voltage of the solar cell. Figure 1 shows an arbitary acceptor impurity profile on a substrate of N_B acceptor atoms per cm^3. The thickness of the p^+-layer is W and the impurity concentration at every point is denoted as $N_A(x)$. The usual way of studying the physical mechanisms underlying the operation of the back surface field of a BSF solar cell is through the introduction of an effective surface recombination velocity (S_{eff}) located at the high–low interface[1]. This S_{eff} takes into account at once the minority carrier behaviour in the highly doped layer when the lowly doped substrate is under study.

S_{eff} is defined as

$$S_{eff} = -\frac{J_e(0^-)}{qn'(0^-)} \tag{1}$$

where $J_e(0^-)$ and $n'(0^-)$ are respectively the electron current and the excess electron concentration at the

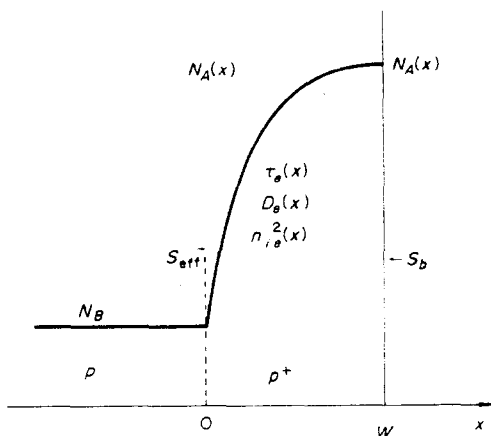

Fig. 1. Impurity profile of a pp^+ high–low junction.

low-side of the pp^+ junction. The distinction between 0^- and 0^+ is made to include the case of an abrupt junction.

After a rigorous study of the equilibrium potential distribution within the space charge region (SCR) of a high–low junction Gunn[14] concluded that the potential drop across the SCR never exceeds kT/q and is almost entirely related to the low region. Hence, one can write

$$J_e(0^-) = J_e(0^+) \tag{2}$$

$$\frac{n(0^-)\cdot p(0^-)}{n^2_{ie}(0^-)} = \frac{n(0^+)\cdot p(0^+)}{n^2_{ie}(0^+)}. \tag{3}$$

The two relations are valid provided that changes in the quasi-Fermi levels across the SCR are negligible and the recombination within the SCR can be neglected.

In the range of doping levels used in actual BSF solar cells heavy doping phenomena have to be taken into account. From an engineering point of view this can be done by means of a rigid bandgap narrowing model[15]. The effective intrinsic concentration becomes position dependent through position dependence of high doping concentration and hence the electron equilibrium concentration, $n_0(x)$, is calculated as

$$n_o(x) = \frac{n^2_{ie}(x)}{N_A(x)} = \frac{n^2_{io}}{N_{Aeff}(x)} \tag{4}$$

where n^2_{io} is the conventional intrinsic concentration and N_{Aeff} is the effective impurity concentration[15].

The combination of eqns (1)–(4) allows to express S_{eff} as

$$S_{eff} = -\frac{J_e(0^+)}{qn'(0^+)}\frac{N_{Beff}}{N_{Aeff}(0^+)} \tag{5}$$

noticing that a quasi-neutral low-injection condition is assumed at the edges of the SCR, and thus $n'(0^-) \simeq n(0^-)$, $n'(0^+) \simeq n(0^+)$, $p(0^-) \simeq N_B$, $p(0^+) \simeq N_A(0^+)$.

The minority carrier current density in the quasi-neutral p^+-region can be written as[16]

$$J_e(x) = qD_e(x)\left[\frac{n'(x)}{N_{Aeff}(x)}\cdot\frac{\mathrm{d}N_{Aeff}(x)}{\mathrm{d}x} + \frac{\mathrm{d}n'(x)}{\mathrm{d}x}\right]. \tag{6}$$

The combination of eqn (6) and the continuity equation

$$\frac{\mathrm{d}J_e(x)}{\mathrm{d}x} = q\frac{n'(x)}{\tau_e(x)} \tag{7}$$

leads to the following differential equation

$$\left(-\frac{J_e}{qn'}\right)^2\frac{1}{D_e} = \frac{-1}{N_{Aeff}}\frac{\mathrm{d}N_{Aeff}}{\mathrm{d}x}\left(-\frac{J_e}{qn'}\right) + \frac{d}{\mathrm{d}x}\left(-\frac{J_e}{qn'}\right) + \frac{1}{\tau_e}. \tag{8}$$

The definition of the new variable

$$S_e(x) = -\frac{J_e(x)}{qn'(x)} \tag{9}$$

simplifies eqn (8) to

$$\frac{dS_e}{dx}=\frac{S_e^2}{D_e}+\frac{S_e}{N_{Aeff}}\frac{dN_{Aeff}}{dx}-\frac{1}{\tau_e}. \quad (10)$$

This first order non linear differential equation takes into account the three main important mechanisms affecting minority carriers: diffusion, drift and recombination. The boundary condition is the recombination velocity at the back contact. The solution of eqn (10) at $x=0^+$ gives $S_e(0^+)$ which is related to S_{eff} through eqns (5) and (9).

In general eqn (10) must be solved numerically. We will consider two particular cases in which analytical solutions can be obtained. For nn^+ high–low junctions eqn (10) is again found but changing the subindexes "e" by "h" and "A" by "D". In the following calculations we will omit the subindexes.

(a) *Abrupt junction*

In this case N_{eff}, D and τ are constant all along the highly-doped side. Equation (10) can easily be integrated since it now becomes

$$\frac{dS}{dx}=\frac{S^2}{D}-\frac{1}{\tau}. \quad (11)$$

Integrating, S_{eff} results to be

$$S_{eff}=\frac{N_{Beff}}{N_{eff}}\frac{D}{L}\frac{\frac{S_bL}{D}+\text{th}\frac{W}{L}}{1+\frac{S_bL}{D}\text{th}\frac{W}{L}} \quad (12)$$

where S_b is the surface recombination velocity. A formula like (12) has been first deduced by Sinha and Chattopadhyaya[17] using the abrupt junction results of Goldlewski *et al.*[1]. Here a more general deduction has been carried out.

(b) *Transparent heavily doped region*

Shibib *et al.*[18] show recently that the emitter dark current of modern solar cells is mainly dominated by recombination at the surface rather than within the bulk of the layer. In certain situations high–low junctions may behave in a similar way.

When recombination in the heavily-doped region can be neglected, eqn (10) becomes

$$\frac{ds(x)}{dx}=\frac{S^2(x)}{D(x)}+\frac{S(x)}{N_{eff}(x)}\frac{dN_{eff}(x)}{dx} \quad (13)$$

This differential equation is now integrable and the solution is

$$S_{eff}=\frac{N_{Beff}}{\int_0^W \frac{N_{eff}(x)}{D(x)}dx+\frac{N_{eff}(W)}{S_b}}. \quad (14)$$

For BSF solar cells $S_b=\infty$ and eqn (14) admits another simplifications step

$$S_{eff}=\frac{N_{Beff}}{\int_0^W \frac{N_{eff}(x)}{D(x)}dx} \quad (15)$$

Equations (14) and (15) are of considerable interest since the integral can be very accurately calculated with a simple pocket calculator, i.e. an error of less than 4% can easely be obtained.

The importance of the integrated doping profile in the base of a BSF solar cell combined with the mobility concentration dependence was already shown by Fossum[3]. However in this work the influence of the weight of the integrated doping profile of the heavily-doped layer on S_{eff} is outlined. This fact allows the study of the base of the solar cell in the conventional way and a deeper physical interpretation of the high–low junction minority carrier reflecting properties will be now feasible.

3. COMPUTER RESULTS

Equation (10) has been numerically solved in the case of a pp^+ high–low junction. A complementary error function profile was selected as the best approximation to a real impurity profile. Experimental concentration dependence results from Conwell[19] were used as mobility data. At every integration step the mobility was calculated taken into account the local impurity concentration and the total electric field. The lifetime model proposed by Kendall[20] and already used by Fossum[21] and Lauwers *et al.*[22] is also used in the present study

$$\tau_e=\frac{12}{1+\frac{N_A}{5\cdot 10^{16}}}\ \mu\text{sec}. \quad (16)$$

The experimentally determined formula of Slotboom and de Graaff[23] is employed here to calculate the effective intrinsic carrier concentration, n_{ie}, at every point of the p^+-layer

$$\Delta V_{go}(N_A)=9\cdot\left[\ln\frac{N_A}{10^{17}}+\sqrt{\left(\ln^2\frac{N_A}{10^{17}}+0.5\right)}\right]\text{mV}. \quad (17)$$

S_{eff} is calculated from eqn (10) as a function of the layer thickness, surface impurity concentration and surface recombination velocity. The results are shown in Figs 2–4. The substrate impurity concentration is $10^{16}\,\text{cm}^{-3}$.

In Fig. 2 an infinite surface recombination velocity is assumed. This is the case for BSF solar cells. Two clearly defined regions can be observed in the 2 and 5 μm curves. First a quite steep decrease of S_{eff} when the surface concentration increases is noticed corresponding to the transparent region. Above some times $10^{20}\,\text{cm}^{-3}$ the S_{eff} saturates. This is due to the increasing recombination in the layer due to lifetime degradation at high doping levels combined with the slower increase of

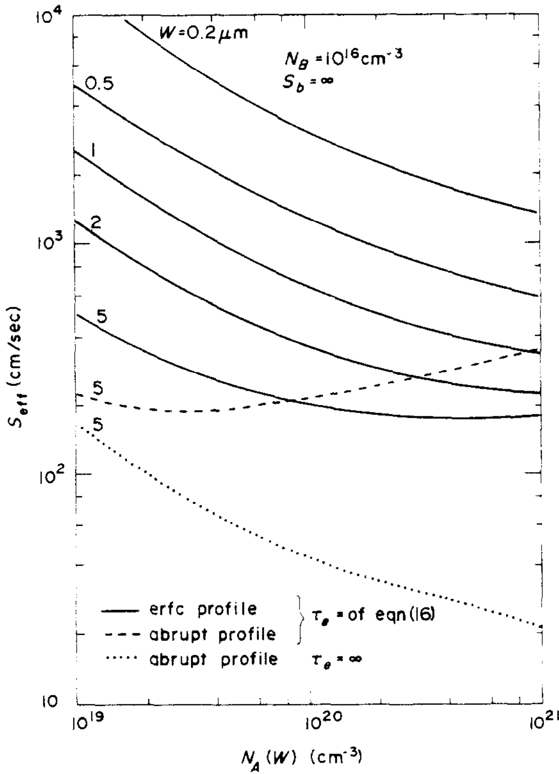

Fig. 2. S_{eff} of erfc pp^+ high–low junctions as a function of the surface concentration and the layer-thickness ($S_b = \infty$).

the integrated effective impurity doping profile caused by the bandgap narrowing. In narrower p^+-regions this second mechanism is not so important because of the reduced recombination volume.

A saturation rather than an optimum point is found when the surface impurity concentration is increased. This result is in contradiction with [17]. This discrepancy arises from the fact that the abrupt profile considered in [17] overestimates the influence of the degraded lifetime with respect to the most real erfc profile. In Fig. 2 the broken line gives the S_{eff} of an abrupt profile with a minority carrier lifetime given by eqn (16). The dotted line represents the same case, but with infinite lifetime. The comparison of these two curves indicates that the bandgap narrowing would not be responsable for the existence of an optimum doping level in an abrupt high–low junction.

Figure 3 plots the calculated S_{eff} when different surface recombination velocities are considered at the surface of a 1 μm thick p^+-layer. For high S_b the S_{eff} decreases with increasing surface concentration since the recombination at the back contact is the main recombining mechanism (quasi-transparency). This effect is predicted by eqn (14). For low S_b however the recom-

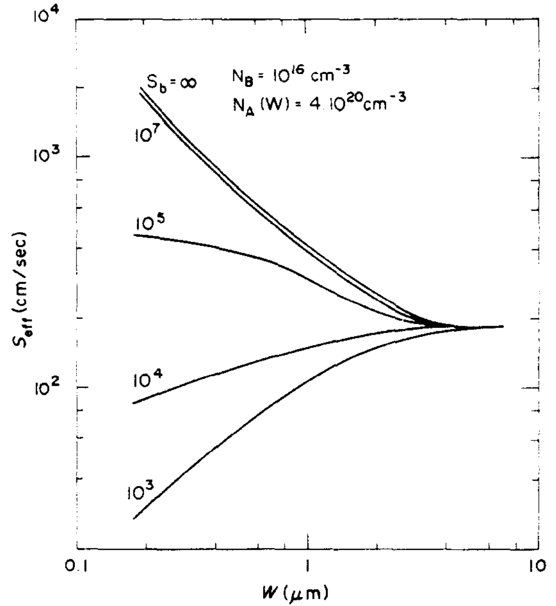

Fig. 4. S_{eff} as a function of the layer thickness and the surface recombination velocity ($N_A(W) = 4.10 \cdot 10^{20}$ cm^{-3}).

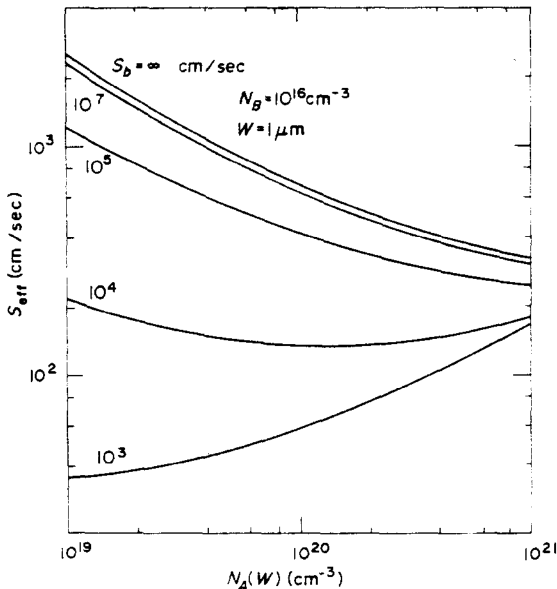

Fig. 3. S_{eff} as a function of the surface concentration and the surface recombination velocity ($W = 1$ μm).

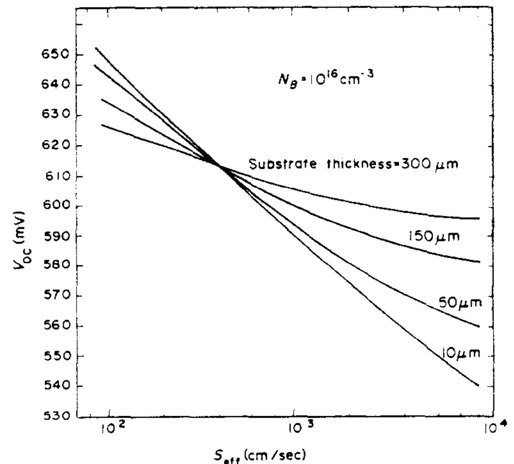

Fig. 5. V_{oc} as a function of S_{eff} and the base thickness of a BSF solar cell ($L = 882$ μm [20], $D = 23.3$ cm^2/sec [19]).

bination within the layer is dominant and hence as the doping level increases the lifetime progresively degrades and S_{eff} increases.

In Fig. 4, S_{eff} is plotted as a function of the layer thickness and of the surface recombination velocity for a typical surface concentration of $4 \cdot 10^{20}\,cm^{-3}$. When the p^+-layer is very thick all the injected minority carriers recombine within the bulk of the heavily doped layer and a small number of them reach the surface. In this region of total "opacity" the S_{eff} is independent of surface treatments.

To clarify the concepts of "transparency" and "opacity" and to determine the range of application of eqns (14) and (15) we introduce a *transport factor*, α_T, analogous to the transport factor in the base of a transistor. α_T is defined as the minority carrier current reaching the back contact divided by the current injected into the layer

$$\alpha_T = \frac{J(W)}{J(0)}. \qquad (18)$$

The use of this parameter provides more physical insight than the transit time used by Shibib *et al.*[18]. In their case the definition of a mean lifetime is required to be compared with the transit time and establish where the recombination mainly takes place. The problem of defining a mean lifetime in an inhomogeneously doped region is avoided with the definition of the transport factor.

Table 1 collects the calculated transport factor of two extreme cases and the different results obtained for S_{eff} from the exact computer simulation, eqn (10) and (14). α_T illustrates the use of eqn (14).

4. IMPLICATIONS ON SOLAR CELL DESIGN

BSF solar cell design is quite well established[2, 3]. However further remarks can be made from the numerical results obtained earlier. Fossum's conclusion[3] that in the presence of an infinitely recombining contact at the back of the cell, increasing the surface concentration much above $10^{19}\,cm^{-3}$ and the thickness of the highly doped back layer more than $0.5\,\mu m$ does not improve solar cell performance, seems to be too optimistic.

We have calculated the dark saturation current of the base of a solar cell[24] with an impurity concentration of $10^{16}\,cm^{-3}$ as a function of the recombination velocity at the back surface. Assuming negligible recombination in the emitter and a short-circuit current of $30\,mA/cm^2$ (AM1) the corresponding open-circuit voltage has been deduced. It is plot in Fig. 5 for several base thicknesses.

Table 1. Data and results of two typical opac and transparent erfc pp^+ high–low junctions.

Layer characteristics			S_{eff}(cm/sec)			
$W(\mu m)$	$N_A(W)$ $\times(cm^{-3})$	S_b(cm/sec)	exact	eqn (10)	eqn (14)	α_T
0.2	$4 \cdot 10^{20}$	∞	2127	1919	1969	0.95
5	$4 \cdot 10^{20}$	∞	217	207	85	0.14

To reach an upper limit of 615 mV, which is the value obtained for a good emitter, at least an S_{eff} of 300 cm/sec must be present at the back contact, independently of the layer thickness. Such a low S_{eff} can only be technologically feasible by means of a highly doped layer at least $2\,\mu m$ thick and a surface concentration of $10^{20}\,cm^{-3}$, or $5\,\mu m$ thick and $3 \cdot 10^{19}\,cm^{-3}$ surface concentration. The discrepancy is a major effect of bandgap narrowing since no one kind of heavy doping effects were included in the modelling made at [3]. Our more restricted experimental lifetime model of [20] can also influence the final result. Measurements recently reported [25] on high-efficient BSF solar cells confirm our expectations.

It has been proposed that partial coverage of the back contact of a BSF solar cell can provide a lower back surface recombination velocity and decrease the S_{eff} of the high-low junction[13]. However this will not improve the open-circuit voltage of the solar cell if the BSF were already efficient. This can be concluded from the combination of Figs 3 and 5. In the case of a highly-doped layer with a surface concentration of $4 \cdot 10^{20}\,cm^{-3}$ and a thickness of $1\,\mu m$ as shown in Fig. 3, S_{eff} will decrease from 420 to 290 cm/sec when S_b changes from ∞ to 10^5 cm/sec. This will improve the V_{oc} less than 5 mV (Fig. 5). Only a further passivation to lower the S_{eff} down to 100 cm/sec will improve the total efficiency of the BSF solar cell provided that the emitter is good enough. However a surface recombination smaller than 10^3 cm/sec cannot be obtained on a surface with an impurity concentration of $4 \cdot 10^{20}\,cm^{-3}$. A thin heavily-doped layer rather than a thick one will improve S_{eff} without such an energic passivation of the surface. Figure 4 opens this possibility if the layer thickness is $0.3\,\mu m$ and $S_b = 10^4$ cm/sec. A further optimization of the surface impurity concentration will be necessary as stated in Fig. 3.

To lower the emitter recombination current a high–low emitter has been proposed [7, 8]. In Fig. 5 the V_{oc} of a $10\,\mu m$ thick high–low emitter with a low-side impurity concentration of $10^{16}\,cm^{-3}$[8] is presented as a function of the S_{eff} of the front high–low junction. To have an increase of the open-circuit voltage further than 620 mV again an effective surface recombination velocity smaller than 300 cm/sec must be reached. Since the thickness of the highly-doped layer must be kept as thin as possible such an S_{eff} is only achieved if a passivation of 10^4 cm/sec at the surface is feasible, as we concluded in the previous paragraph. The technological problems involved in passivation of heavily doped surfaces have not been solved. In fact no more than 625 mV at 25°C (AMO conditions) have been obtained from a diffused – HLE cell[8].

Lammert and Schwartz proposed the Interdigitated Back Contact Solar Cell for operation at high concentration levels[26]. The absence of a front grid pattern and the considerable reduction in the series resistance due to the back contact are its major advantages. For the correct operation of the IBC cell two important conditions must be fulfilled: a high-lifetime bulk and a low front surface recombination velocity. In the case of a bulk

lifetime of 1000 μsec the front surface recombination velocity should be lower than 32 cm/sec if a 90% of the maximum conversion efficiency wants to be reached[26]. To achieve such a low number von Roos and Anspaugh proposed the fabrication of a high–low junction at the front surface[10]. From Fig. 4 we can conclude that an erfc p^+ layer of $4.10^{20}\,cm^{-3}$ surface concentration could provide the adequate S_{eff} if the thickness of the p^+-layer is at least 0.8 μm. We assume that a recombination velocity of 10^5 cm/sec is attained at the surface. This conclusion applies for a 14 Ω/cm ($N_B = 10^{15}\,cm^{-3}$) substrate, necessary to obtain long lifetimes. With the aid of eqn (5), we see that the S_{eff} of this case is one tenth of the S_{eff} when $N_B = 10^{16}\,cm^{-3}$.

A double sided BSF solar cell (DSSF) was proposed by Luque *et al.*[9] to be used in conjunction with low-concentration quasi-static systems. As for the FSF solar cell the collection efficiency of this structure is very sensitive to the value of the effective surface recombination velocity of the high–low junction. On 14 Ω cm p-type substrate exact computer simulations indicate that S_{eff} should be lower than 42 cm/sec. A 0.5 μm thick p^+-layer could only provide the required S_{eff} if it is doped at least up to $4.10^{20}\,cm^{-3}$. No one practical value of surface concentration seems to be possible with layers thinner than 0.4–0.5 μm if surface passivation is not available.

5. CONCLUSIONS

A simple theoretical model to calculate the effective surface recombination velocity of an arbitrary high–low junction allows to design high–low junctions for solar cells. When the high–low junction is located at a non-illuminated surface, like in the case of BSF solar cell, the tendency is to obtain smaller S_{eff}'s when the high–low junction is thickner and more heavily doped. There is not an optimum value of surface impurity concentration. However if passivation of the heavily doped surface is available a thinner and lower doped profile and selective metal contact on the surface can further reduce the S_{eff}.

For high–low junctions located on illuminated surfaces the effort must be concentrated on passivation of the surface. The reason is that the lower the surface recombination velocity the thinner the highly doped side is required for obtaining a given desired S_{eff}. An optimum surface impurity concentration is shown to appear depending on the degree of passivation achieved.

Acknowledgements—The authors thank Prof. R. van Overstraeten for critically reviewing portions of this work. We acknowledge enthusiastic encouragement from Profs A. Luque and J. Eguren.

REFERENCES

1. M. P. Godlewski, C. R. Baraona and H. W. Brandhorst, Jr. *Proc. 10th IEEE Phot. Spec. Conf*, p. 40. Palo Alto (1973).
2. J. R. Hauser and P. M. Dunbar, *IEEE Trans. Electron Dev.* **ED-24**, 305 (1977).
3. J. G. Fossum, *IEEE Trans. Electron Dev.* **ED-24**, 322 (1977).
4. J. Mandelkorn and J. H. Lamneck, Jr., *Proc. 9th IEEE Phot. Spec. Conf.*, p. 66. New York (1972).
5. J. Mandelkorn and J. H. Lamneck, Jr., *Proc. 11th IEEE Phot. Spec. Conf.*, p. 36. Scottsdale (1975).
6. J. G. Fossum and E. L. Burgess, *Appl. Phys. Lett.* **33**, 238 (1978).
7. C. T. Sah, F. A. Lindholm and J. G. Fossum, *IEEE Trans. Electron Dev.* **ED-25**, 66 (1978).
8. F. A. Lindholm, A. Neugroschel, S. C. Pao, J. G. Fossum and C. T. Sah, *Proc. 13th IEEE Phot. Spec. Conf.*, p. 1300. Washington (1978).
9. A. Luque, A. Cuevas and J. Eguren, *Solid-St. Electron* **21**, 793 (1978).
10. O. von Roos and B. Anspaugh, *Proc. 13th IEEE phot. Spec. Conf.*, p. 1119. Washington (1978).
11. J. R. Hauser and P. M. Dunbar, *Solid-St. Electron.* **18**, 715 (1975).
12. A. Sinha and S. K. Chattopadhyaya, *Solid-St. Electron.* **21**, 943 (1978).
13. J. G. Fossum, R. D. Nasby and E. L. Burgess, *Proc. 13th IEEE Phot. Spec. Conf.* p. 1294, Washington (1978).
14. J. B. Gunn, *J. Electron. Control* **4**, 17 (1958).
15. H. J. de Man, *IEEE Trans. Electron Dev.* **ED-18**, 833 (1971).
16. R. J. van Overstraeten, H. J. de Man and R. P. Mertens, *IEEE Trans. Electron Dev.* **ED-20**, 290 (1973).
17. A. Sinha and S. K. Chattopadhyaya, *IEEE Trans. Electron Dev.* **ED-25**, 1412 (1978).
18. M. A. Shibib, F. A. Lindholm and F. Therez, *IEEE Trans. Electron. Dev.* **ED-26**, 959 (1979).
19. E. M. Conwell, *Proc. IRE* **46**, 1281 (1958).
20. D. Kendall, *Conf. Physics and Appl. of Li Diffused Silocon.* NASA-Goddard Space Flight Center (Dec. 1969).
21. J. G. Fossum, *Solid-St. Electron* **19**, 269 (1976).
22. P. Lauwers, J. van Meerbergen, P. Bulteel, R. Mertens and R. van Overstraeten, *Solid-St. Electron* **21**, 747 (1978).
23. J. W. Slotboom and H. C. de Graaff, *Solid-St. Electron.* **19**, 857 (1976).
24. H. J. Hovel, *Solar Cells*, p. 52. Academic Press, New York (1975).
25. H. T. Weaver and R. D. Nasby, *Solid-St. Electron.* **22**, 687 (1979).
26. M. D. Lammert and R. J. Schwartz, *IEEE Trans. Electron Dev.* **ED-24**, 337 (1977).